Effect of Ceria Nanoparticles on the Corrosion Inhibition of Pectin for X60 Steel in HCl Solution

Saviour A. Umoren

Centre of Research Excellence in Corrosion, Research Institute, King Fahd University of Petroleum and Minerals, Dhahran 31261, Kingdom of Saudi Arabia

Email: umoren@kfupm.edu.sa

ABSTRACT

Ceria (CeO_2) nanoparticles were synthesized and characterized using scanning electron microscopy (SEM), powder x-ray diffraction (XRD), attenuated total reflectance infrared (ATR-IR) spectroscopy and thermogravimetric analysis (TGA) techniques. The effect of addition of the synthesized CeO_2 on the corrosion inhibition effect of pectin for X60 steel in 0.5 M HCl solution was evaluated using electrochemical impedance spectroscopy (EIS), potentiodynamic polarization and weight loss techniques at 25 and 60 ^oC. Water contact angle measurements, scanning electron microscopy and ATR-IR techniques were employed for surface morphology characterization. Results obtained show that both CeO_2 and pectin acts as moderate corrosion inhibitors for X60 steel in the acid environment. Inhibition efficiency increased with increase in the additives concentration. Inhibition efficiency of pectin was enhanced on addition of CeO_2 due to synergistic effect especially at ambient temperature and higher concentration of CeO_2. Temperature was found to have profound effect on the corrosion inhibition performance of pectin without and with addition of CeO_2. The potentiodynamic polarization studies revealed that Pectin, CeO_2 and Pectin-CeO_2 mixtures functions as a mixed-type inhibitor. Results from all the surface analyses confirm the formation of protective film on the X60 steel surface.

Keywords: Pectin; Ceria; Nanoparticles; Acid corrosion; Corrosion inhibition; Synergism

1. Introduction

Low carbon steel of different grades is essential commodity in the chemical and petrochemical industries. The major setback of steel is that it corrodes very rapidly when it comes in contact with aggressive acid solutions if used without adequate protection. Hydrochloric acid is heavily deployed in industrial applications such as acid pickling, acid cleaning of boilers, descaling of boilers and oil well acidizing [1, 2]. In order to prevent the base metal attack and reduce excessive acid consumption during these processes, corrosion inhibitors are widely employed [3]. In recent times, the most important criteria in selecting corrosion inhibitors for practical application apart from efficiency is the eco-friendliness of the inhibitor because of problems of environmental pollution. In this regards, the search has been focused on the use of rare earth metals as green alternative for chromium. Similarly biopolymers have been advocated as alternative for toxic organic inhibitors. Among the rare earth compounds, cerium salts/ions have been reported to inhibit the corrosion of steel, galvanized steel and non-ferrous alloys either by coatings or as inhibitors [4 –10]. On the other hand, biopolymers are readily available as their sources are abundant; they are low cost, renewable and robust compared to their synthetic counterparts. They are also ecofriendly and benign, and possess optimal biocompatibility and biodegradability. Umoren and Eduok in their recent reviews have documented biopolymers that have been reported as corrosion inhibitors for metal substrates in different corrosive media [11].

However, the use of single compound as corrosion inhibitor has the disadvantage of high amount of usage. In this regard, the combination of two or more compounds which often show a

synergistic behavior is advocated. The advantage is that it leads to a reduction of the amount of inhibitor usage and also improves the corrosion inhibition effect of the inhibitor at low concentration [12]. Reports abound in the literature on the synergistic corrosion inhibition effect between organic compounds and halides ions, metal cations and so forth. Recently, Umoren and Solomon have published a review paper on the synergistic corrosion inhibition effect between organic species and halide ions for metal substrates in different corrosive environments [13]. The corrosion inhibition performance of pectin with propyl phosphonic acid (PPA) and Zn^{2+} for corrosion control of carbon steel in neutral aqueous solution has been reported [14]. Also the effect of addition of cerium ions on the corrosion inhibition performance of polyaniline for iron in 0.5 M H_2SO_4 has been reported by Jeyaprabha *et al*. [1]. Similarly, Sasikumar *et al*. [15] have reported that CeO_2 nanoparticles – polyaniline composites could serve as inhibitor for mild steel corrosion in HCl medium. The synergistic effect of the rare-earth cerium (IV) ion and 3, 4-dihydroxybenzaldehye (DHBA) for steel corrosion inhibition in sulfuric acid solution was investigated by Li *et al.* [16]. Forsyth *et al.* [17] studied the synergistic effect of rare earth Ce^{3+} and sodium salicylate for inhibition of corrosion of mild steel in 0.1 M sodium chloride solution. The report on the synergistic inhibition effect of cerium (IV) ion and sodium molybdate for cold-rolled steel in HCl solution by Mu *et al*. [18] is available in the literature.

There is no report to the best of our knowledge on the effect of addition of ceria nanoparticles on the corrosion inhibition performance of pectin for low carbon steel in acid media. Therefore in continuation of our quest to explore biopolymers as eco-friendly corrosion inhibitors and ways of improving/enhancing their performances, the present work reports synergistic corrosion inhibition effect between CeO_2 nanoparticles and pectin for a typical X60 pipeline steel in 0.5 M HCl using weight loss and electrochemical techniques; completed by surface morphological characterization and water contact angle measurements.

2. Experimental Procedures

2.1 Materials and Materials Preparation

The corrosive medium was 0.5 M HCl prepared from 36% analytical grade HCl (Eurostar Scientific Ltd, UK) with doubled distilled water. X60 steel specimens with the chemical composition (weight percentage) as previously reported [14] were used in the experiments. Test coupons for weight loss and electrochemical measurements were cut into 3 cm × 3 cm × 0.25 cm dimensions. These coupons were abraded with silicon carbide paper (from grade #320 to #800), rinsed with distilled water, placed in an ultrasonic acetone bath for about 5 min to remove possible residue of polishing, rinsed with acetone, dried in warm air and then stored in moisture-free desiccators prior to use. Pectin from apple having molecular weight of 75,000 g mol^{-1} and degree of esterification of 65 – 70% was used as test inhibitor in the concentration range of 50 to 500 ppm. CeO_2 nanoparticles was prepared from the precursors ammonium cerium (IV) nitrate and NaOH with 1:4 molar ratios and then characterized using SEM, TGA, XRD and ATR-IR techniques.

2.2 Electrochemical measurements

Electrochemical corrosion tests were performed on electrodes cut from the X60 steel sheet (working electrode). The exposed area of the working electrode to the corrosive acidic medium was 0.7855 cm^2 cm. The exposed surface was also cleaned as described above. Electrochemical cell was a single compartment electrochemical cell designed for mounting varieties of flat samples with three-electrode system. A saturated calomel electrode (SCE) was the reference electrode and all reported potential values are referred to this type of electrode. A graphite rod was used as counter electrode. Experiments were carried out under stagnant aerated conditions at 25 ±1 ^oC.

Measurements were performed using Gamry potentiostat/galvanostat/ZRA (Reference 3000) embedded with Gamry framework system composed of ESA410. Electrochemical impedance spectroscopy (EIS) tests were performed at the end of 30 min immersion at 25 $\pm$ 1°C. Measurements were made at corrosion potential (E_{corr}) over a frequency range of 100 kHz – 100 mHz, with a signal amplitude perturbation of 10 mV. The data were analyzed with Echem Analyst 6.0. The polarization study was from cathodic potential of −250 mV to anodic potential of +250 mV with respect to the corrosion potential at a sweep rate of 1 mV/s. The linear Tafel segments of the anodic and cathodic curves were extrapolated to corrosion potential to obtain the corrosion current densities (i_{corr}). Each experiment was carried out three times to estimate reproducibility and average values of the electrochemical parameters are reported.

2.3 Weight loss measurements

Weight loss the test was conducted in a glass reaction vessel containing 250 mL of test solution maintained at 25 and 60 ^{o}C with thermostated water bath in order to evaluate the effect of temperature on the corrosion inhibition efficacy of pectin and pectin-CeO_2 mixtures. Tests were performed under total immersion in the absence and presence of the inhibitors. In each experiment, duplicate samples of the cleaned and weighed steel coupons were freely suspended in the different test solutions. The test coupons were retrieved after 24 h immersion, thoroughly cleaned using previously reported procedures [19], rinsed with distilled water and acetone and dried in warm air and reweighed using digital analytical balance with sensitivity ± 0.1 mg. The weight loss was taken as the difference between the weight at a given time and the initial weight of the coupon. The data of the triplicate determinations showed good reproducibility and the average values are reported. From the weight loss values, corrosion rates in terms of thickness loss (mm y^{-1}) were computed accordingly using the expression:

$$C_R\,(\text{mm y}^{-1}) = \frac{87.6 \times \Delta W}{\rho A T} \qquad (1)$$

where C_R is the corrosion rate, W is the average weight loss (mg) , ρ is the density of mild steel specimen (g cm^{-3}), A is the surface area of the specimen (cm^2) and T is the exposure time (h).

The inhibition efficiency (η%) of pectin was evaluated from the following equation:

$$\eta\% = \frac{C_{R(blank)} - C_{R(inh)}}{C_{R(blank)}} \times 100 \qquad (2)$$

where $C_{R(blank)}$ and $C_{R(inh)}$ are the corrosion rate in the absence and presence of the inhibitors respectively in 0.5 M HCl at the same temperature.

2.4 Surface morphology analysis

The metal surface was abraded successively using emery papers of grades 400, 600, 800 and 1000. Next, the specimen was fine polished using diamond paste to obtain a mirror- like shiny surface. After polishing, the working electrode was washed with ethanol, rinsed several times with distilled water and, finally dried with hot air. Surface characterization of metal surface, after exposure in the test corrosion medium with and without inhibitors, was carried out using scanning electronic microscope (SEM; JEOL JSM 66100 LV). Water contact angle measurements were conducted at X60 pipeline steel surfaces uncorroded and corroded in 0.5 M HCl in the absence and

presence of 500 and 500 ppm pectin + 5 mM CeO_2 after 24 h immersion at 25 ^oC. The contact angles of a drop of water (3 µL) on steel were measured by sessile drop method with Attension Contact Angle Meter (Biolin Scientific Instrument).

3. Results and discussion

3.1 Synthesis and characterization of CeO_2 nanoparticles

Figure 1 (a-d) displays the SEM image, ATR-IR spectrum, XRD patterns and thermogravimetric profiles respectively of CeO_2 nanoparticles. The SEM showed that synthesized CeO_2 nanoparticles exhibited non-spherical morphology with the diameter of about 10–15 nm. The ATR-IR spectrum displays bands such as 400-600 cm^{-1} , 820–1400 cm^{-1} 2630–3000 cm^{-1}, and 834 cm^{-1} which is typical of CeO_2 [20]. From the XRD pattern, CeO_2 nanoparticles displayed five major peaks at 28.7, 33.2, 47.7, 56.5 and 59.10°, which corresponds to (111), (200), (220), (311) and (222) planes of face-center cubic CeO_2 (JCPDS 78-0694). The thermogram of nano CeO_2 specifies three stage weight losses. In the first stage, 8–10% weight loss at temperature 100 °C is attributed to the loss of water molecules from the synthesized products. The weight loss at second stage that starts above 300 °C (about 5%) is basically due to the removal of dopants and unused precursors. From the TGA results, it can be deduced that the CeO_2 particles are found to be pure and thermally stable with almost no weight loss over the entire range of temperature [21].

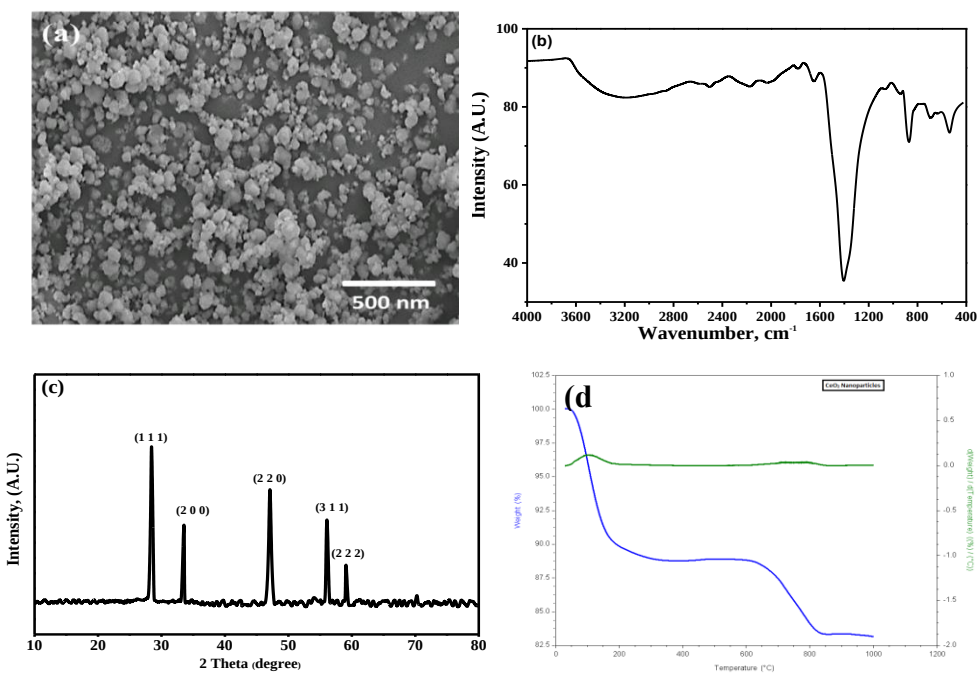

Figure 1: (a) SEM image, (b) ATR-IR spectrum, (c) XRD patterns and (d) thermogravimetric profiles of synthesized CeO_2 nanoparticles

3.2 Corrosion inhibition by pectin and CeO_2 nanoparticles

The corrosion inhibition of X60 steel in 0.5 M HCl without and with different concentrations of pectin (50 – 500 ppm) and CeO_2 nanoparticles (1 – 5 mM) alone was evaluated using electrochemical methods at 25 ^oC. Figure 2 shows the typical potentiondynamic polarization curves for X60 steel in 0.5 M HCl in the absence and presence of different concentrations of (a) pectin and (b) CeO_2 nanoparticles. The important corrosion kinetic parameters viz. corrosion potential (E_{corr}), the corrosion current density (I_{corr}), anodic and cathodic Tafel slopes (β_a and β_c) as well as corrosion rate obtained from these curves are given in Table 1.

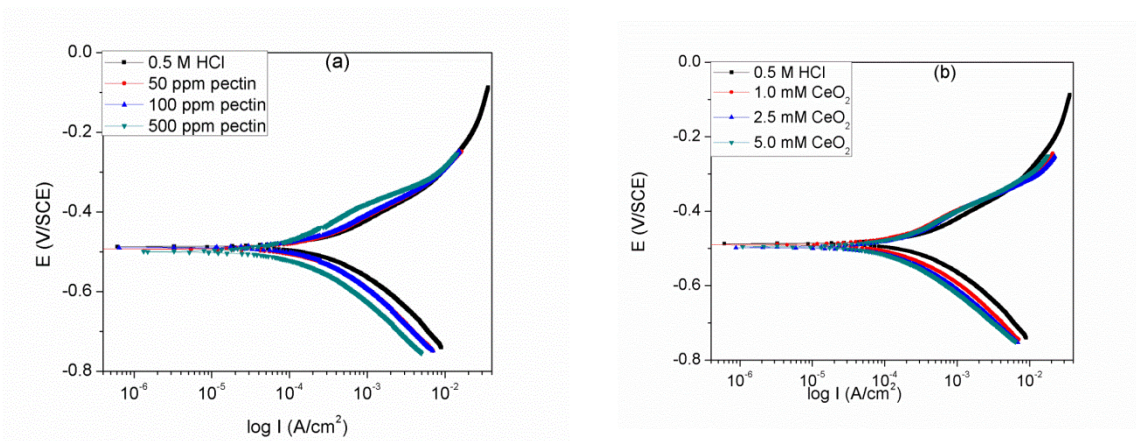

Figure 2: Polarization curves for X60 steel in 0.5 M HCl in the absence and presence of different concentrations (a) pectin (b) CeO_2 at 25 ^oC.

Inspection of Figure 2 shows that the X60 steel underwent active dissolution in the corrosive medium both in the absence and presence of the additives (pectin and CeO_2) without distinctive transition to passivation within the range of the applied potential. From Table 1, it is clearly seen that the corrosion potential (E_{corr}) shifts slightly to the less noble values in the presence of both pectin and CeO_2 in comparison to the blank. However, the difference in E_{corr} values between the optimum investigated concentration of both pectin and CeO_2 and the blank is less than ±85 mV/SCE, which is regarded as a threshold value for an inhibitor to be classified as anodic or cathodic inhibitor. The implication is that both pectin and CeO_2 act as mixed type inhibitor with predominant influence on suppressing the cathodic hydrogen reaction than the anodic metal dissolution reaction. Inhibition efficiency (IE %) was computed from the potentiodynamic polarization technique using the equation (3) and the values obtained are listed in Table 1.

$$IE(\%) = \left(1 - \frac{i_{corr}}{i^0_{corr}}\right) \times 100 \qquad (3)$$

where i^0_{corr} and i_{corr} are the corrosion current densities in the absence and presence of the inhibitors respectively. IE% values listed in Table 1 are seen to increase with increase in concentration of the additives reaching the maximum values of 70.0 and 69.9% at concentrations of 500 ppm pectin and 5 mM CeO_2 respectively.

Table 1: Polarization parameters for X60 steel in 0.5 M HCl in the absence and presence of different concentrations of pectin and CeO_2 nanoparticles at 25 ^oC.

Inhibitor concentration	E_{corr} (mV/SCE)	I_{corr} (μA cm^{-2})	β_a (mV dec^{-1})	β_c (mV dec^{-1})	Corrosion rate (mpy)	*IE* (%)
Blank	–487	277	112	133	161	–
50 ppm pectin	–493	183	104	127	107	33.9
100 ppm pectin	–490	174	102	126	101	37.2
500 ppm pectin	–500	83	115	99	48	70.0
1.0 mM CeO_2	–490	123	92.4	106.9	71.6	55.6
2.5 mM CeO_2	–498	94.4	80.0	99.2	54.9	65.9
5.0 mM CeO_2	–495	83.5	68.5	105.1	48.6	69.9

The impedance plots for X60 steel in 0.5 M HCl in the absence and presence of different concentrations of pectin is shown in Figure 3 in (a) Nyquist and (b) Bode modulus representations. Similar plots in the absence and presence of different concentrations of CeO_2 are depicted in Figure 4 (a) and (b) respectively. It is seen that the Nyquist curves (Fig. 3a and 4a) displayed a single capacitive loop, indicating that they each contained one time constant in the Bode plot. The shapes of the semicircles in the Nyquist plots in the presence of the inhibitors are similar that of the blank solution; implying that the corrosion mechanism was unchanged by the introduction of the inhibitors into the corrosive medium [22].

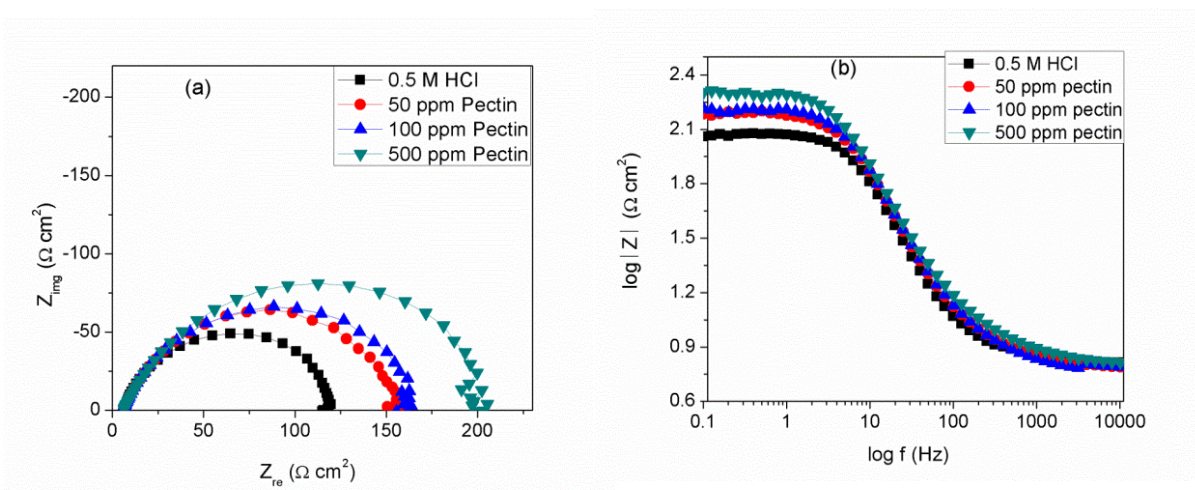

Figure 3: Impedance plots for X60 steel in 0.5 M HCl in the absence and presence of different concentrations pectin at 25 ^oC in (a) Nyquist (b) Bode modulus representations

The shapes of the semicircles in the Nyquist plots in the presence of the inhibitors are similar that of the blank solution; implying that the corrosion mechanism was unchanged by the introduction of the inhibitors into the corrosive medium [23]. In order to deduce the electrochemical parameters of interest, the EIS experimental data was modelled using the equivalent circuit previously reported [24].

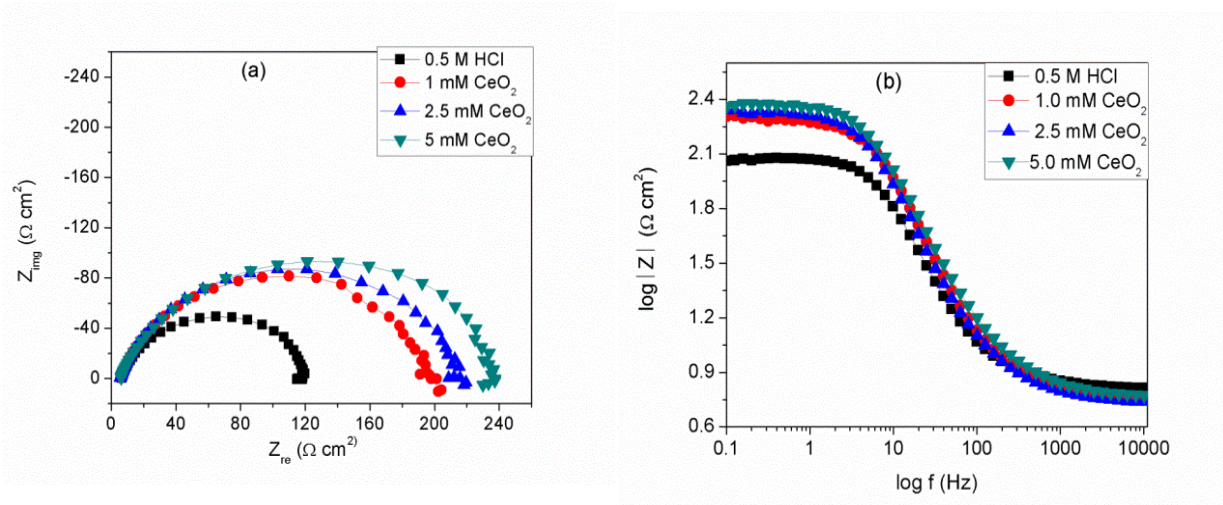

Figure 4: Impedance plots for X60 steel in 0.5 M HCl in the absence and presence of different concentrations pectin at 25 ^{o}C in (a) Nyquist (b) Bode modulus representations

Table 2: Electrochemical impedance parameters for X60 steel in 0.5 M HCl in the absence and presence of different concentrations of pectin and CeO_2 nanoparticles at 25 ^{o}C.

Inhibitor concentration	R_s (Ω cm^2)	R_{ct} (Ω cm^2)	Q ($\mu\Omega$ s^n cm^{-2})	n	C_{dl} (uF cm^2)	$\chi^2 \times 10^{-4}$	IE (%)
Blank	6.6	114.9	237.0	0.87	139.5	8.1	-
50 ppm pectin	6.2	153.7	239.6	0.83	130.4	9.3	25.2
100 ppm pectin	6.0	161.1	236.9	0.83	124.4	12.9	28.7
500 ppm pectin	6.6	203.6	238.0	0.81	123.7	14.6	43.6
1.0 mM CeO_2	5.7	194.6	164.1	0.86	103.0	6.4	40.9
2.5 mM CeO_2	5.5	212.9	185.6	0.85	94.2	5.9	46.0
5.0 mM CeO_2	5.8	235.7	164.6	0.84	85.0	5.9	51.3

The electrochemical parameters derived from the fittings are recorded in Table 2. Results in Table 2 show that the introduction of the additives into the corrosive medium increased the magnitude of the R_{ct} as exemplified by the increase in the diameter of the Nyquist semicircles compared to the blank solution. This is attributed to the formation of the protective film at the steel/solution interface. It is also seen in the table that R_{ct} values increased with increase in concentration of both pectin and CeO_2. The goodness of fit (χ^2) values is low and the range of the values obtained indicates that the equivalent circuit provided a good fit to the experimental data. The inhibition efficiency from the EIS technique was calculated by comparing the R_{ct} values in the absence and presence of pectin and CeO_2 as follows:

$$IE(\%) = \left(1 - \frac{R_{ct}^0}{R_{ct}}\right) \times 100 \qquad (4)$$

where R_{ct}^0 and R_{ct} are the charge transfer resistances in the absence and presence of the inhibitors. The calculated values are also listed in Table 2. It is clear from the results presented in the table

that the corrosion inhibition efficiency increased progressively with increasing inhibitors concentration; reaching the maximum values of 43.6 and 51.3% at the optimum investigated concentrations of pectin (500 ppm) and CeO_2 (5 mM) respectively. The results given in the table also revealed that the addition of the inhibitors to the corrodent leads to a decrease in C_{dl} values. This observation have been generally linked to a decrease in the dielectric constant and/or an increase in double layer thickness as a consequence of adsorption of the inhibitor (which is assumed to have lower dielectric constant compared to the displaced adsorbed water molecule) onto the steel/solution interface, hence protecting the metal from corrosion [25].

3.3 Effect of CeO_2 addition on corrosion inhibition performance by pectin

The effect of addition of CeO_2 on the corrosion inhibition effect of pectin was assessed using electrochemical techniques. Figure 5 shows potendiodynamic polarization curves for X60 steel in 0.5 M HCl without, with pectin (500 ppm) and pectin in combination with different concentrations (1, 2.5 and 5 mM) CeO_2 at 25 ^{o}C. The corrosion kinetic parameters derived for the polarization curves are listed in Table 3. It is noted from the results obtained (Fig. 6 and Table 3) that the corrosion potentials were not affected by the addition of CeO_2 to pectin. From Table 3, the corrosion current density is observed to increase from 83 to 119 µA cm^{-2} on addition of 1 mM CeO_2 to 500 ppm pectin whereas a decrease in corrosion current density from 83 to 73 and 68 µA cm^{-2} could be observed on addition of 2.5 and 5 mM CeO_2 respectively comparison to the same concentration of pectin. In a corresponding manner, inhibition efficiency decreased from 70 to 57 % on addition of 1 mM CeO_2 and marginally increased from 70.0 to 73.7 and 75.4% on addition of 2.5 and 5 mM CeO_2 respectively to 500 ppm pectin.

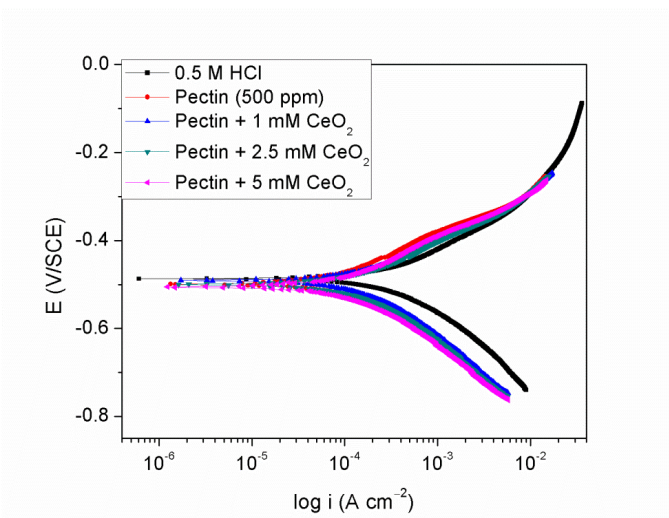

Figure 5: Polarization curves for X60 steel in 0.5 M HCl in the absence and presence of pectin and pectin-CeO_2 mixtures at 25 ^{o}C.

Table 3: Polarization parameters for X60 steel in 0.5 M HCl in the absence and presence of pectin (500 ppm) and pectin in combination with CeO_2 nanoparticles at 25 ^oC.

Inhibitor concentration	E_{corr} (mV/SCE)	I_{corr} (μA cm^{-2})	β_a (mV dec^{-1})	β_c (mV dec^{-1})	Corrosion rate (mpy)	IE (%)
Blank	–487	277	112	133	161	–
pectin (500 ppm)	–500	83	115	99	48	70.0
Pectin + 1 mM CeO_2	–491	119	79	129	69	57.0
Pectin + 2.5 mM CeO_2	–500	73	67	83	42	73.7
Pectin + 5 mM CeO_2	–506	68	86	93	40	75.4

The effect of addition of CeO_2 on the corrosion inhibition performance of pectin was also investigated using EIS technique. Figure 6 shows the representation of the complex impedance of X60 steel in 0.5 M HCl in the absence and presence of 500 ppm pectin and this concentration of pectin in combination with different concentrations of CeO_2 in (a) Nyquist and (b) Bode modulus formats. As noted in individual (pectin and CeO_2) inhibited solutions, the Nyquist curves are characterized by single capacitive loop which also corresponds to one time constant in the Bode modulus format. Inspection of the Nyquist plots also revealed that the shape of the curves in the presence of pectin and pectin – CeO_2 mixtures remains the same indicating that the addition of CeO_2 to pectin did not alter the mechanism of the corrosion process.

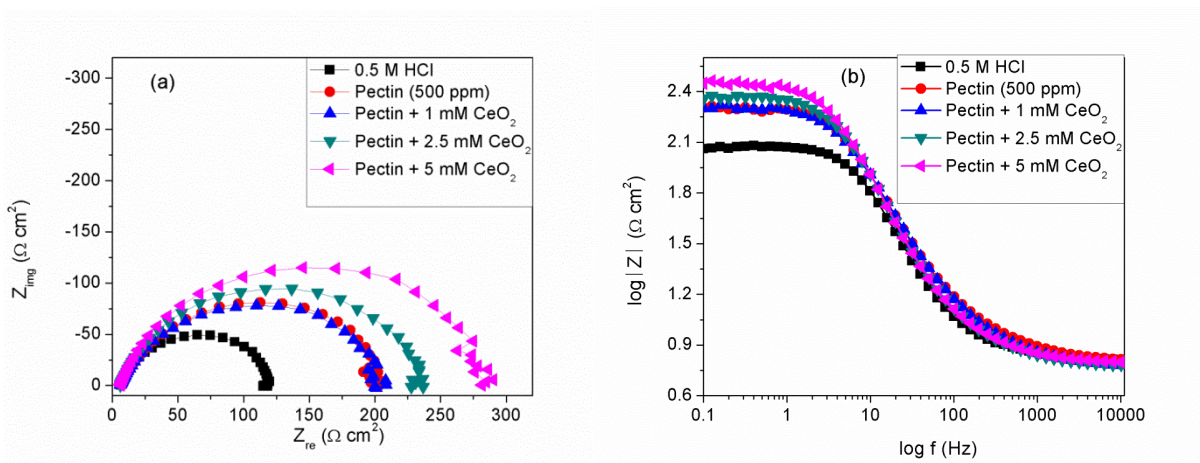

Figure 6: Impedance plots for X60 steel in 0.5 M HCl in the absence and presence of pectin and pectin-CeO_2 mixtures at 25 ^oC.

The same equivalent circuit used earlier was also used to fit the experimental data for pectin – CeO_2 mixtures and the electrochemical parameters generated are listed in Table 4. It is clear from Table 4 that the R_{ct} is increased in the presence of pectin alone compared to the blank and further increased in the presence of pectin – CeO_2 combination especially at higher concentration of CeO_2. Examination of Table 4 also revealed that C_{dl} values in the presence of the additives are lower than that of the blank. The decrease in C_{dl} in the presence of inhibiting agent is often attributed to the decrease in local dielectric constant and /or an increase in the thickness of the electrical double layer as a result of adsorption of the inhibitors on the metal surface [1]. The inhibition efficiency values listed in Table 4 are observed to follow the trend reported for potentiodynamic polarization

measurements and are seen to increase in the mixed inhibitor systems particularly with increase in CeO_2 concentration.

Table 4: Electrochemical impedance parameters for X60 steel in 0.5 M HCl in the absence and presence of pectin (500 ppm) and pectin in combination with CeO_2 nanoparticles at 25 ^oC.

Inhibitor concentration	R_s (Ω cm^2)	R_{ct} (Ω cm^2)	Q ($\mu\Omega$ s^n cm^{-2})	n	C_{dl} (μF cm^2)	$\chi^2 \times 10^{-4}$	IE (%)
Blank	6.6	114.9	237.0	0.87	139.5	8.1	–
pectin (500 ppm)	6.6	203.6	238.0	0.81	123.7	14.6	43.6
Pectin +1 mM CeO_2	5.99	203.7	244.6	0.81	123.6	9.6	43.6
Pectin + 2.5 mM CeO_2	6.08	234.3	204.8	0.84	135.6	7.3	51.0
Pectin + 5 mM CeO_2	6.32	284.1	193.4	0.85	111.8	5.9	60.0

In order to determine the nature of effect existing between pectin and CeO_2 used as inhibitors for X60 steel in 0.5 M HCl, the synergistic parameter (S_1) was calculated using the equation initially proposed by Aramaki and Hackerman [26] and thereafter reported by many researchers [1,27] as follows:

$$S_1 = \frac{1-(\eta_1+\eta_2)}{1-\eta_{1+2}} \quad (5)$$

where η_1 is the inhibition efficiency of pectin, η_2 is the inhibition efficiency of CeO_2 and η_{1+2} is the measured inhibition efficiency for pectin in combination with CeO_2. $S_1 > 1$ points to synergistic effect of the selected inhibitors combination whereas $S_1 < 1$ and $S_1 = 1$ indicates antagonistic effect and no interaction between the two inhibitors respectively. The calculated values of the synergistic parameter from EIS and PDP measurements are given in Table 5. It is evident from Table 5 that the values are greater than unity and are seen to be more pronounced for PDP than EIS method. This indicates that the enhanced corrosion inhibition effect of pectin particularly on addition of increased amount of CeO_2 is due to synergistic effect. The pronounced values of the synergistic parameter observed from PDP measurements compared to EIS measurements is consistent with the trend of inhibition efficiency values obtained from the two techniques which is also more pronounced for PDP technique

Table 5: Synergism Parameter (S_1) for different concentrations of CeO_2 at 25 ^oC from electrochemical impedance spectroscopy (EIS) and potentiodynamic polarization (PDP) measurements

CeO_2 concentration (mM)	Synergism parameter (S_1)	
	PDP method	EIS method
1.0	2.23	1.95
2.5	1.85	1.78
5.0	1.88	1.59

3.4 Effect of Temperature

Temperature is an important kinetic factor that influences the corrosion rate of metal and modifies the adsorption of inhibitor on electrode surface. In order to assess the effect of temperature on the corrosion inhibition performance of pectin and pectin – CeO_2 mixtures, weight loss experiments were conducted at 25 and 60 ^oC using the optimum concentrations of both pectin and CeO_2 studied. The values of weight loss, corrosion rate, degree of surface coverage (θ) and inhibition efficiency obtained from the weight loss measurements at the two temperatures investigated are listed in Table 5. From Table 6, it is apparent that weight loss and corrosion rate of X60 steel in 0.5 M HCl decreased in the presence of pectin compared to the blank solution and further decreases in the solution containing pectin – CeO_2 mixtures at 25 ^oC. However, at 60 ^oC, weight loss and corrosion rate values are observed to increase in the presence of pectin – CeO_2 mixtures compared to pectin alone. Further inspection of Table 5 reveals that in the absence and presence of the additives, weight loss and corrosion rate increased with increase in temperature. Inhibition efficiency is seen to increase from 62.9 to 94.0% as the temperature was raised from 25 to 60 ^oC in the presence of pectin alone and from 87.6 to 91.3% respectively with pectin – CeO_2 mixtures. The increase in inhibition efficiency with increase in temperature is largely attributed to chemisorption mechanism involving interaction of de-localized electrons of inhibitor molecules and vacant, low energy d-orbitals of Fe surface atoms [27].

Table 6: Calculated values of weight loss, corrosion rate, inhibition efficiency and surface coverage for X60 steel in 0.5 M HCl in the absence and presence of pectin (500 ppm) and pectin-CeO_2 mixtures different temperatures.

Temperature (^oC)	System/concentration	Weight loss (mg)	Corrosion rate (mm/yr)	Inhibition efficiency	Surface coverage (θ)
	Blank	96.4	5.16	–	–
25	500 ppm pectin	35.8	2.06	62.9	0.63
	500 ppm + CeO_2	12.0	0.52	87.6	0.88
	Blank	1260.7	65.01	–	–
60	500 ppm pectin	75.3	4.13	94.0	0.94
	500 ppm + CeO_2	109.3	5.68	91.3	0.91

The apparent activation energy for the X60 steel corrosion without and with pectin and pectin – CeO_2 mixtures was determined from weight loss measurements from Arrhenius equation as follows:

$$E_a = 2.303R(\log\frac{1}{C_{R2}} - \frac{1}{C_{R1}})\left(\frac{T_2T_1}{T_2 - T_1}\right) \quad (6)$$

where C_{R1} and C_{R2} are the corrosion rates at temperatures T_1 and T_2 respectively and R is the molar gas constant. The heat of adsorption was also estimated from the weight loss data based on the trend of surface coverage with temperature the as follows:

$$Q_{ads} = 2.303R\left[\log\left(\frac{\theta_2}{1-\theta_2}\right) - \log\left(\frac{\theta_1}{1-\theta_1}\right)\right] \times \left(\frac{T_1T_2}{T_2 - T_1}\right) \quad (7)$$

where θ_1 and θ_2 are the degrees of surface coverage at temperatures T_1 and T_2. The calculated values of both the activation energy and heat of adsorption are listed in Table 7. Results in Table 7 show that activation energy was lowered in the presence of pectin and pectin-CeO_2 mixtures

compared to the uninhibited solution. This is expected given that inhibition efficiency increases with increase in temperature. This phenomenon has been largely attributed to specific interactions between the inhibiting agents and the metal surface [28].

Table 7: Kinetics/thermodynamic parameters for X60 steel in 0.5 M HCl in the absence and presence of pectin and pectin in combination with CeO_2.

System/concentration	E_a (kJ/mol)	Q_{ads} (kJ/mol)
Blank	59.73	–
Pectin (500 ppm)	16.40	52.33
Pectin + 5 mM CeO_2	56.35	7.06

The values of heat of adsorption displayed in Table 7 are positive in the presence of pectin and pectin + CeO_2. The positive values of the heat of adsorption and the corresponding increase in inhibition efficiency with increase in temperature is frequently associated with chemical adsorption mechanism. The reverse corresponding to negative value of heat of adsorption and a decrease in inhibition efficiency with rise in temperature suggests a physisorption mechanism [29].

3.5 Surface analysis

Fig. 7 (a-d) shows the micrographs of X60 steel coupons in (a) unexposed polished state, (b) exposed to the blank solution (0.5 M HCl), (c) immersed in acid solution containing 500 ppm pectin, and (d) exposed to corrosive medium containing 500 ppm pectin + 5 mM CeO_2 for 24 h. In the polished state (Fig. 9(a)), the X60 steel surface appears very smooth but the morphology of the surface changed considerably on exposure to the corrosive medium (Fig. 9(b)). The surface is seen to be rough due to severe attack by the acid. The acid attack is observed to be relatively uniform with no evidence of localized corrosion. In comparison to Fig. 9 (b), the surfaces in Fig. 9(c) and (d) clearly revealed a relatively smooth surface and evident of the adsorbate on the surface. This indicates that the additives reduced the active surface area of the steel exposed to the aggressive medium by virtue of adsorption on the metal surface.

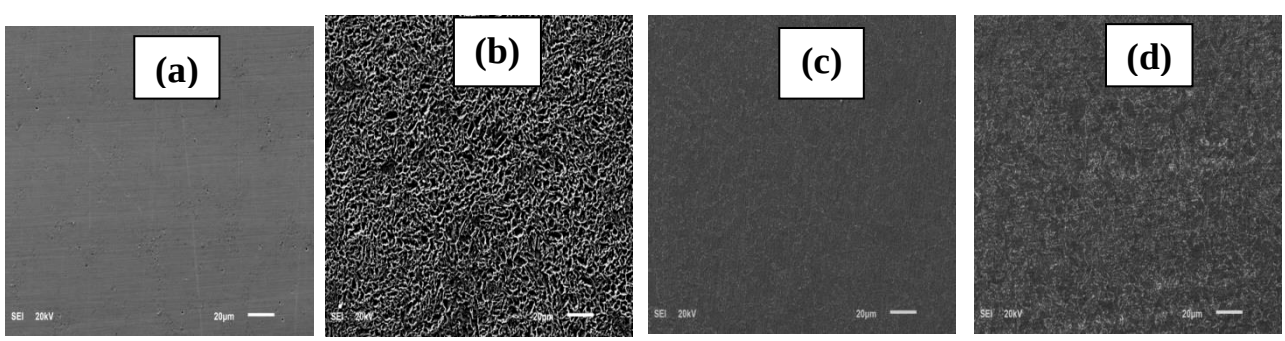

Figure 7: SEM micrographs of X60 steel coupons in (a) unexposed polished state, (b) exposed to 0.5 M HCl, (c)) exposed to 0.5 M HCl containing 500 ppm pectin, and (d)) exposed to 0.5 M HCl containing 500 ppm pectin + 5 mM CeO_2

Fig. 8 depicts the contact angle images of water droplet on X60 steel surfaces (a) in the polished state, (b) exposed to 0.5 M HCl solution, (c) exposed to 0.5 M HCl solution containing 500

ppm pectin and (d) exposed to 0.5 M HCl solution containing 500 ppm pectin + 5 mM CeO_2 for 24 h. From the figure, the values of the contact angles were 89.8°, 86.5°, 106.3° and 118.4° for X60 steel, X60 steel in 0.5 M HCl, X60 steel in 0.5 M HCl containing 500 ppm pectin and X60 steel in 0.5 M HCl containing 500 ppm pectin + 5 mM CeO_2 respectively. It is clear from the results that the contact angles are lower for X60 steel in the polished state and on exposure to 0.5 M HCl compared to the ones in the corrosive medium containing pectin and pectin + CeO_2. This can be attributed to the presence of hydrophilic corrosion products and oxide films on the X60 steel surface which increases the surface wettability [30, 31]. Addition of pectin and pectin + CeO_2 to the corrosive medium is seen to alter the surface wettability of X60 steel significantly resulting in the increase in values of contact angles from 86.5° to 106.3° and 118.4° respectively. The values of the contact angles revealed that the steel surface in the presence of the additives is hydrophobic in nature which undoubtedly attributed to the adsorption of pectin and pectin – CeO_2 mixtures to form a protective film. Also the value of the contact angle of X60 steel in inhibited solution of pectin – CeO_2 mixtures is higher than that of pectin alone confirming the synergistic inhibition effect of CeO_2 addition to pectin.

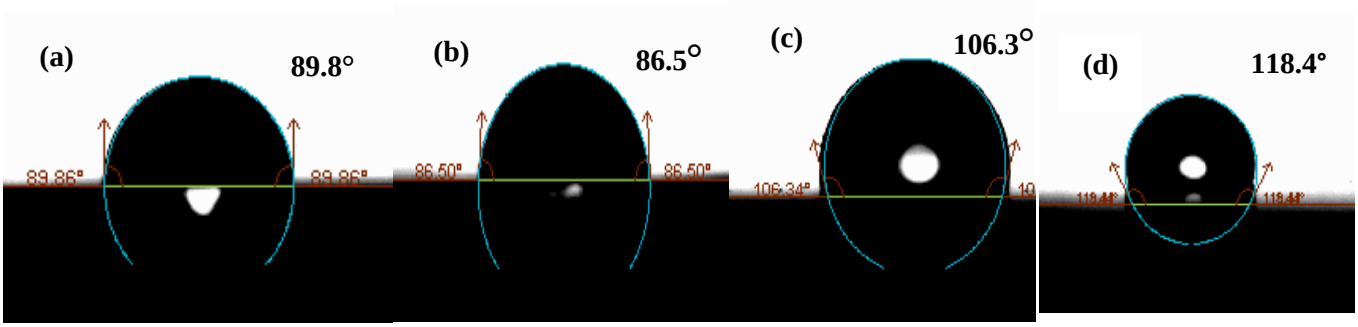

Figure 8: Water contact angles of X60 steel coupons in (a) unexposed polished state, (b) exposed to 0.5 M HCl, (c)) exposed to 0.5 M HCl containing 500 ppm pectin, and (d)) exposed to 0.5 M HCl containing 500 ppm pectin + 5 mM CeO_2

Fig. 9 depicts the IR spectra of pure pectin, film on the metal surface exposed to 0.5 M HCl containing 500 ppm pectin and pectin – CeO_2 mixtures. In the IR spectrum of pure pectin, typical absorption peaks were observed at 3390 cm^{-1} and 2947 cm^{-1} due to an O-H stretching vibration and the C-H stretching of the CH_2 group, respectively. Further, the two bands observed at 1618 and 1435 cm^{-1} were attributed to vibrations of the O-C-O structure. The band at 1735 cm^{-1} is ascribed to the C-O stretching vibration of methyl esterified carboxylic group. In addition, C-H bending and C-O stretching was obtained at 1310 cm^{-1} and 1300–1000 cm^{-1} respectively [24]. Comparing the pure spectrum of pectin with the spectrum of 500 ppm of pectin adsorbed on steel, it is evident that almost all the peaks in the pure pectin sample are present in the surface film formed on the steel surface. In addition, Pectin in combination with CeO_2 nanoparticles also exhibited the peaks of pure pectin and CeO_2 nanoparticles which further confirm the surface film formed on the steel surface.

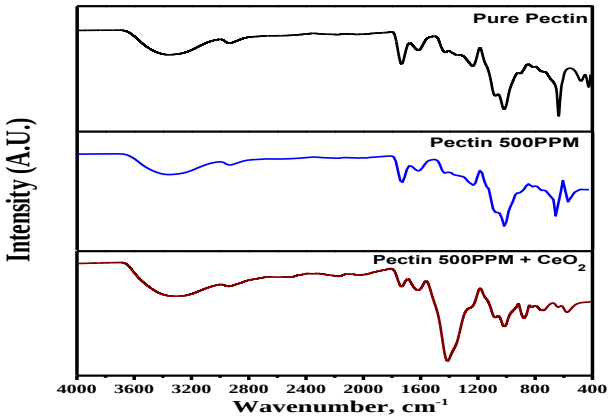

Figure 9: IR spectra of pure pectin, film on the metal surface exposed to 0.5 M HCl containing 500 ppm pectin and 500 ppm pectin + 5 mM CeO_2

4. Conclusions

From the results obtained, the following conclusions can be drawn from the work.

1. Pectin and CeO_2 act as moderate corrosion inhibitors for X60 steel in 0.5 M HCl environment. Inhibition efficiency increased with increase in pectin and CeO_2 concentration and also increased as the temperature is raised.
2. Addition of CeO_2 to pectin enhanced the inhibitive ability of pectin due to synergistic effect particularly at higher concentrations of CeO_2. The synergistic effect was confirmed from the calculated values of synergistic parameter (S_1) which was found to be greater than unity.
3. Potentiodynamic polarization results revealed that pectin alone and in combination with CeO_2 functions as mixed type corrosion inhibitors.
4. AT-IR, SEM and water contact angles measurements results points clearly to the fact that pectin alone and in combination with CeO_2 were adsorbed onto the metal surface to form protective films.

Acknowledgements

The author gratefully acknowledged King Fahd University for Petroleum and Minerals (KFUPM) for sponsorship and Centre of Research Excellence in Corrosion, KFUPM for supporting the work.

References

[1] C. Jeyaprabha, S. Sathiyanarayanan, G. Venkatachari, Effect of cerium ions on corrosion inhibition of PANI for iron in 0.5 M H_2SO_4, Applied Surface Science, 253 (2006) 432-438.
[2] F. El-Taib Heakal, N.S. Tantawy, O.S. Shehata, Influence of cerium (III) ions on corrosion and hydrogen evolution of carbon steel in acid solutions, International Journal of Hydrogen Energy, 37 (2012) 19219-19230.
[3] M. El Azhar, B. Mernari, M. Traisnel, F. Bentiss, M. Lagrenée, Corrosion inhibition of mild steel by the new class of inhibitors [2,5-bis(n-pyridyl)-1,3,4-thiadiazoles] in acidic media, Corrosion Science, 43 (2001) 2229-2238.

[4] C. Wang, F. Jiang, F. Wang, The characterization and corrosion resistance of cerium chemical conversion coatings for 304 stainless steel, Corrosion Science, 46 (2004) 75-89.
[5] M.F. Montemor, A.M. Simões, M.G.S. Ferreira, Composition and behaviour of cerium films on galvanised steel, Progress in Organic Coatings, 43 (2001) 274-281.
[6] M.A. Arenas, J.J. de Damborenea, Growth mechanisms of cerium layers on galvanised steel, Electrochimica Acta, 48 (2003) 3693-3698.
[7] M.A. Arenas, A. Conde, J.J. de Damborenea, Cerium: a suitable green corrosion inhibitor for tinplate, Corrosion Science, 44 (2002) 511-520.
[8] B.R.W. Hinton, Corrosion inhibition with rare earth metal salts, Journal of Alloys and Compounds, 180 (1992) 15-25.
[9] A. Aldykewicz, H. Isaacs, A. Davenport, The investigation of cerium as a cathodic inhibitor for aluminum-copper alloys, Journal of the Electrochemical Society, 142 (1995) 3342-3350.
[10] P. Rodič, I. Milošev, Corrosion inhibition of pure aluminium and alloys AA2024-T3 and AA7075-T6 by cerium (III) and cerium (IV) salts, Journal of the Electrochemical Society, 163 (2016) C85-C93.
[11] S.A. Umoren, U.M. Eduok, Application of carbohydrate polymers as corrosion inhibitors for metal substrates in different media: A review, Carbohydrate Polymers, 140 (2016) 314-341.
[12] M. Mobin, S. Zehra, R. Aslam, L-Phenylalanine methyl ester hydrochloride as a green corrosion inhibitor for mild steel in hydrochloric acid solution and the effect of surfactant additive, RSC Advances, 6 (2016) 5890-5902.
[13] S.A. Umoren, M.M. Solomon, Effect of halide ions on the corrosion inhibition efficiency of different organic species - A review, Journal of Industrial and Engineering Chemistry, 21 (2015) 81-100.
[14] M. Prabakaran, S. Ramesh, V. Periasamy, B. Sreedhar, The corrosion inhibition performance of pectin with propyl phosphonic acid and Zn^{2+} for corrosion control of carbon steel in aqueous solution, Res Chem Intermed, 41 (2015) 4649-4671.
[15] Y. Sasikumar, A.M. Kumar, Z.M. Gasem, E.E. Ebenso, Hybrid nanocomposite from aniline and CeO2 nanoparticles: Surface protective performance on mild steel in acidic environment, Applied Surface Science, 330 (2015) 207-215.
[16] X. Li, S. Deng, H. Fu, G. Mu, Synergistic inhibition effect of rare earth cerium(IV) ion and 3,4-dihydroxybenzaldehye on the corrosion of cold rolled steel in H_2SO_4 solution, Corrosion Science, 51 (2009) 2639-2651.
[17] M. Forsyth, C.M. Forsyth, K. Wilson, T. Behrsing, G.B. Deacon, ATR characterisation of synergistic corrosion inhibition of mild steel surfaces by cerium salicylate, Corrosion Science, 44 (2002) 2651-2656.
[18] G.N. Mu, X.H. Li, Q. Qu, J. Zhou, Synergistic effect on corrosion inhibition by cerium (IV) ion and sodium molybdate for cold rolled steel in hydrochloric acid solution, Acta Chimica Sinica, 62 (2004) 2386-2390.
[19] S.A. Umoren, Z.M. Gasem, I.B. Obot, Natural products for material protection: Inhibition of mild steel corrosion by date palm seed extracts in acidic media, Industrial and Engineering Chemistry Research, 52 (2013) 14855-14865.
[20] M. Taguchi, S. Takami, T. Adschiri, T. Nakane, K. Sato, T. Naka, Supercritical hydrothermal synthesis of hydrophilic polymer-modified water-dispersible CeO_2 nanoparticles, CrystEngComm, 13 (2011) 2841-2848.
[21] A. Madhan Kumar, M. Mizanur Rahman, Z.M. Gasem, A promising nanocomposite from CNTs and nano-ceria: Nanostructured fillers in polyurethane coatings for surface protection, RSC Advances, 5 (2015) 63537-63544.
[22] M. Taguchi, S. Takami, T. Adschiri, T. Nakane, K. Sato, T. Naka, Supercritical hydrothermal synthesis of hydrophilic polymer-modified water-dispersible CeO_2 nanoparticles, Cryst Eng Comm, 13 (2011) 2841-2848.

[23] X. Li, S. Deng, X. Xie, Experimental and theoretical study on corrosion inhibition of oxime compounds for aluminium in HCl solution, Corrosion Science, 81 (2014) 162-175.
[24] S.A. Umoren, I.B. Obot, A. Madhankumar, Z.M. Gasem, Performance evaluation of pectin as ecofriendly corrosion inhibitor for X60 pipeline steel in acid medium: Experimental and theoretical approaches, Carbohydrate Polymers, 124 (2015) 280-291.
[25] M.H. Hussin, M.J. Kassim, The corrosion inhibition and adsorption behavior of Uncaria gambir extract on mild steel in 1 M HCl, Materials Chemistry and Physics, 125 (2011) 461-468.
[26] K. Aramaki, N. Hackerman, Inhibition mechanism of medium-sized polymethyleneimine, Journal of the Electrochemical Society, 116 (1969) 568-574.
[27] M. Mobin, S. Zehra, R. Aslam, L-Phenylalanine methyl ester hydrochloride as a green corrosion inhibitor for mild steel in hydrochloric acid solution and the effect of surfactant additive, RSC Advances, 6 (2016) 5890-5902.
[28] A. Popova, M. Christov, A. Vasilev, Mono- and dicationic benzothiazolic quaternary ammonium bromides as mild steel corrosion inhibitors. Part III: Influence of the temperature on the inhibition process, Corrosion Science, 94 (2015) 70-78.
[29] E.E. Oguzie, Evaluation of the inhibitive effect of some plant extracts on the acid corrosion of mild steel, Corrosion Science, 50 (2008) 2993-2998.
[30] X. He, Y. Jiang, C. Li, W. Wang, B. Hou, L. Wu, Inhibition properties and adsorption behavior of imidazole and 2-phenyl-2-imidazoline on AA5052 in 1.0 M HCl solution, Corrosion Science, 83 (2014) 124-136.
[31] V. Pandarinathan, K. Lepková, S.I. Bailey, T. Becker, R. Gubner, Adsorption of corrosion inhibitor 1-dodecylpyridinium chloride on carbon steel studied by in situ AFM and electrochemical methods, Industrial and Engineering Chemistry Research, 53 (2014) 5858-5865.